

# Two-dimensional full wavefield tomography of wide-angle seismic data from the Faeroe Basin

CATERINA CHIRONI (c.chironi@ic.ac.uk), JOANNA MORGAN (j.v.morgan@ic.ac.uk), MIKE WARNER (m.warner@ic.ac.uk), C.H. TONG (ch.tong@ic.ac.uk) and IVAN STEKL (i.stekl@ic.ac.uk)

Department of Earth Science and Engineering, Imperial College, London, UK

## Introduction

Where near-normal incidence seismic imaging of sub-basalt regions is problematic, the physical properties of the rocks in the subsurface concerned can be constrained through the investigation of the seismic wavefield at long offset. To retrieve this information, analysis of the full wavefield may be required. Here the full wavefield method, based on the numerical solution of the wave equation using the finite-difference approach, is employed. It is based on an iterative optimisation of the waveform misfit between observed and model-generated data, where the latter are calculated from a starting velocity model or that from previous iterations. The wavefield inversion has been formulated in various domains including time-space, Tau-P and frequency-space; the frequency-space formulation developed by Pratt et al. (1998) is used here. Velocity images produced using full wavefield tomography have a resolution of the order of the seismic wavelength, comparable to that of migrated, normal-incidence data.

## Faeroe Basin data

The seismic data investigated here were acquired in 1998 in the Faeroe Basin by Veritas DGC Ltd. The survey was carried out using two ships, one carrying the source and a 12 km streamer, the other a 5 km streamer. Shot and receiver spacing were 75 and 25 m respectively. This geometry enabled acquisition of data up to 18 km of offset, although only data up to 12 km have been analysed so far. Five seismic phases were interpreted to build a starting velocity model for the wavefield inversion: (1) refractions from sediments above the basalts; (2) top-basalt reflections; (3) turning rays from the basalts; (4) bottom-basalt reflections; and (5) basement reflections. Travel-times were modelled using a 2-D inverse algorithm (Zelt and Smith, 1992). The starting model for travel-time modelling was based on previous tomographic results (Carpenter, 2000). The final velocity model consisted of four layers, from top to bottom: (a) sediments with  $V_P$  ranging from 1.7 to 2.3 km/s; (b) basalts around 2 km thick with  $V_P$  from 4.8 to 5.2 km/s; (c) sediments with  $V_P$  from 3.7 to 3.9 km/s; and (d) basement with  $V_P$  of about 6 km/s at the top.

## Method

Having constructed a starting model that matched the interpreted travel-times, we investigate the potential of the wavefield inversion code for resolving basalt and sub-basalt structures. Synthetic data, calculated by superimposing different types of velocity anomaly on this starting model, were inverted to test the resolution in each part of our model, enabling the optimisation of parameters and evaluation of the best strategy for the inversion. A minimum-phase source signature with dominant frequency 14 Hz was extracted from the real data and used in the modelling. A top-down procedure, in which the shallow velocity structure was matched first followed by increasingly deeper part of the model, was adopted. Lower frequencies were inverted first to mitigate the non-linearity in the inversion. A finite-difference grid spacing of 14.8 m was selected on the basis of the minimum velocity and maximum frequency content in the data. Frequencies between 5 and 21 Hz were chosen for the inversion by analysing the frequency spectrum of the real data and according to the offset range used (Sirgue and Pratt, 2000). Three tests performed on the synthetic data are described and results discussed. First, squared checkerboard anomalies of different sizes representing sinusoidal velocity perturbations of 1-10% with respect to the background velocity were superimposed on the top sedimentary layer and synthetic data calculated, and inverted using the unperturbed case as starting model. Second, to test the recovery of the basalt-sediment interface, a single basalt layer extending to the base of the model was used as the starting model. Third, low-velocity layers were included in the basalt unit to simulate velocity variations likely to exist between natural basalt lithologies.

## Results and conclusion

Results from the first test show that inversion successfully recovered both velocity perturbations and anomalies (Fig. 1a). Checkerboard anomalies are better recovered in regions where the wave coverage is good. In the second test, the location and polarity of the discontinuity at the base of the basalt was also recovered (Fig. 1b). Test of the third type involving

the inversion of a complex wavefield is currently being performed together with the inversion of real data. In conclusion, our preliminary tests on synthetic data show that wavefield tomography can retrieve velocity anomalies within and beneath basalts.

## References

Carpenter, M. E., 2000. Seismic imaging using densely sampled, very long-offset data, MPhil thesis, University of Cambridge.

Pratt, R. G., Shin, C. and Hicks, G., 1998. Gauss-Newton and Newton methods in frequency-space seismic waveform inversion, *Geophysical Journal International*, **133**, 341-352.

Sirgue, L. and Pratt, R.G., 2000. Frequency Domain Waveform Inversion: A strategy for choosing frequencies, Expanded abstract, 63<sup>rd</sup> Conference European Association of Geoscientist and engineers.

Zelt, C. and Smith, R., 1992. Seismic traveltime inversion for 2-D crustal velocity structure, *Geophysical Journal International* **108**, 16-34.

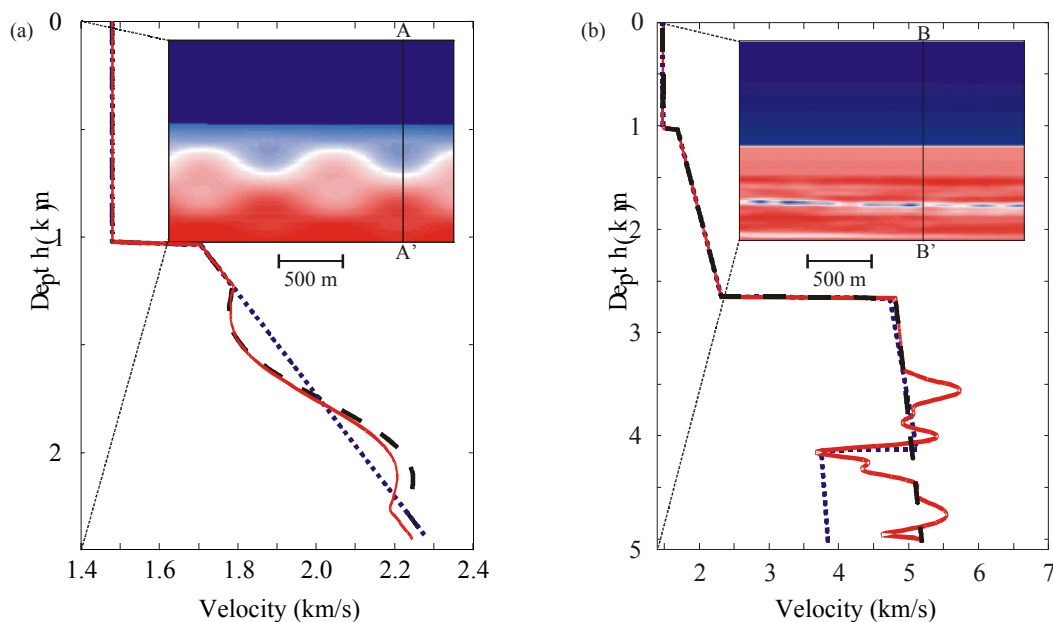


**Figure 1: Test results for wavefield inversion of synthetic data. Velocity functions are slices through the 2-D recovered velocity model from the first test (a) across AA'; and the second test (b) across BB'. The top-right pictures display a close-up of the recovered model. Dot-dashed lines represent the starting model. Dashed lines indicate the model to be recovered. Solid lines show the recovered velocity model.**